

# Effect of Sharp Corners' Nozzles on Inverse Jet Diffusion Flames

M. A.Nosier<sup>#1</sup>, M.M.Kamal<sup>#2</sup>, M.A.Khalek<sup>#2</sup>, A.M.Hamed<sup>#2</sup>; G.El Gamal<sup>\*3</sup>

<sup>#1</sup>Future University, Faculty of Engineering and Technology, Mechanical Engineering Department,

<sup>#2</sup>Ain Shams University, Faculty of Engineering, Mechanical Power Department,

<sup>\*3</sup>Heliopolis University, Faculty of Engineering, Mechatronics Department.

## Abstract

Reactants mixing has great effect on the combustion efficiency, the use of sharp corners in nozzles is recently investigated as an approach to obtain better mixing conditions for inverse jet diffusion flames and to generate a fully developed flame having low unburned hydrocarbons. The present work examines the effect of using nozzles with sharp corners on inverse jet diffusion flames experimentally. This research has been held for reacting flow, using nine different sharp corners nozzles with an approximate equivalent diameter of 12.38 mm. Circular nozzle is adopted as a reference value for comparison. The experiments were held at a constant air to fuel ratio of 50.30. The obtained results showed that increasing the number of sharp corners led to an increase of 38.54 % in the temperature fluctuations. Consequently, there was a reduction of 13.78 % in the peak temperature using the cross nozzle and an increase of 30% for the octagon nozzle. The triangular nozzle showed an effective enhancement in the fuel to air mixing rates such that the flame length was shortened by 50 %.

**Keywords** \_Turbulence, Jet, Flame, Sharp Corner, Diffusion, Inverse jet

## Nomenclatures:

$\rho$  = Density, kg/m<sup>3</sup>

$c_p$  = specific heat capacity, J/kg.K

$\nu$  = Kinematic Viscosity, m<sup>2</sup>/s

$\kappa$  = thermal conductivity of air, W/m.K

$\alpha$  = thermal diffusivity, m<sup>2</sup>/s

$T_p$  = temperature of the probe, K

$x$  = axial distance measured from nozzle, m

$q_c$  = conduction heat transfer, J

$q_r$  = radiation heat transfer, J

$h_c$  = convective heat transfer coefficient, W/m<sup>2</sup>.K

$A$  = surface area, m<sup>2</sup>

$\varepsilon$  = Emissivity

$\sigma$  = Stefan-Boltzmann's constant ( $5.67 \times 10^{-8}$  W m<sup>-2</sup> K<sup>-4</sup>)

## I. INTRODUCTION

There is always a direct impact of turbulence on both combustion rates and flame stability limits which

can be favourably modulated to increase the thermal loading, minimize pollutants and to establish reliable firing techniques. Different methods are used to improve the combustion efficiency and stability. One of these techniques is replacing the circular fuel nozzles with non-circular fuel nozzles. Examine the effects of different non-circular cross section nozzle shapes on the flame characteristics were investigated [1- 20]

Increasing the number of corners of non-circular fuel nozzles led to increasing the number of turbulence production locations, while the smaller vertex angles settled a more severe potential for flow strain around these corners. The interaction between the two overlapped boundary layers at each corner pronounced a favorably increased velocity gradient which acted as a productive center of turbulence [1].

The loss of jet axi-symmetry at the exit causes generally the mean velocity decaying faster, and the fluctuating intensity growing, in the near flow field, thus indicating the increased overall entrainment rate. Asymmetric nozzles reduced the jet flame liftoff height, and consequently they stabilize the flame base closer to the nozzle compared with conventional circular nozzles. Furthermore, the reattachment velocity is nearly identical for all nozzles, which is an indication that nozzle geometry does not significantly influence the reattachment process. [2, 7]

Several issues were common to all noncircular shapes; they included axis switching and the azimuthal variation of the shear-layer spreading rate and turbulence production. The evolution of the jets was shown to depend strongly on initial conditions at the nozzle exit. It included parameters such as the initial azimuthal momentum thickness distribution at the nozzle lip, the ratio of shear-layer-thickness to jet equivalent diameter, the local shear-layer curvature, the eccentricity measured by the nozzle geometrical aspect ratio, Reynolds and Mach numbers, and the jetto-background velocity and density ratios. These initial conditions determine the structure of the asymmetric vortices that roll up in the near jet field. As the vortices convect downstream, vortex deformation and self-induction processes control the downstream evolution of the jet, leading under certain conditions to the axis-

switching phenomenon. The increased entrainment characteristics and enhanced fine-scale mixing of noncircular jets are the result of complex interactions between azimuthal and stream-wise vortices, which are unique to this type of flow field, [6].

The studies showed that, for equal jet cross-sections, reducing the vertex angle from 90° to 30° increases the peak turbulent kinetic energy to 6.27 times due to intensification via mutual diffusion. Whereas, the flame temperature fluctuations varies between 10% and 22.8% as the sharp corner port changes among these different shapes [1]. Triangular ports increase air entrainment by 30%, decrease nitrogen oxides emission by less than 15%, and increase carbon monoxide emission by 20%. These effects are explained in terms of the changes in both flow structure and instabilities which is caused by both of the noncircular geometry and sharp corners of the burner exit port [5]. The rectangular nozzle has a much lower flame liftoff height than the other nozzles [7].

The current work is thus commissioned to examine the effect of sharp corners on inverse diffusion jet flames performance, concerning the number of angles, and its sharpness degree having the same cross sectional areas but with nine different geometric shapes of fuel nozzles.

## II. METHODOLOGY

### A. EXPERIMENTAL TEST RIG

Test rig setup was used for an inverse diffusion flame, at a constant air to fuel ratio of 50.30 as a total value distributed as 52.06 for outer race of flame and 2.45 for inner race, where the central air is involved in reaction while the outer air is used for dilution. The test rig shown in Fig.2 consists of a cylindrical combustion chamber Fig. 1, of eight inch diameter and 60 cm length is designed, with ten temperature measuring ports each of ten millimeters diameter (12), and insulated with wool glass sheet coated with aluminum sheet, the combustion chamber is attached to the whole

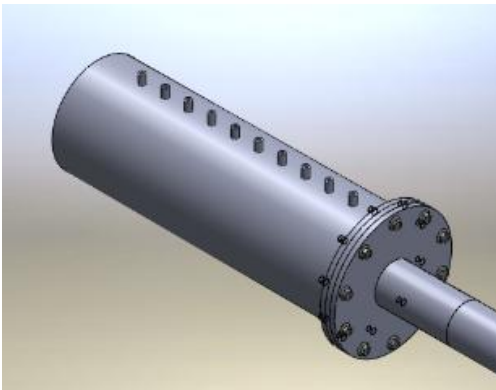


Fig. 1: Combustor scheme

system through ten bolts and nuts size M10 (13). The temperature is measured using S-type thermocouple having 0.5 mm junction diameter, as shown in Fig.2.

The piping system contains two main streams, namely, fuel line and air line. The air-line diameter is three inches and is branched into two lines for inner and outer coaxial flow. While the fuel line diameter is half inch and is fixed between the two air lines through a 90° connection (7). Both air and fuel flow rates are measured through orifice flow meters (9 and 14) using a U-tube manometer for air and an inclined manometer for fuel. And this flow is controlled through two ball valves (15 and 16). As shown in Fig. 2.

Fuel is finally delivered through a nozzle (6), which is designed with nine shapes of different geometry all having the same cross-sectional area of 120 mm<sup>2</sup>, which is reduced by the area of the central air line of seven millimeters outer diameter to become of a value of 81.5 mm<sup>2</sup>. All nozzles cross-section details are presented in table(1). Air is supplied through a blower (18) of 60cm blower diameter and 1.5 H.P., while L.P.G. fuel cylinder (17) is of 40% C<sub>3</sub>H<sub>8</sub> and 60% C<sub>4</sub>H<sub>10</sub>, with a pressure regulator valve (20). As shown in Fig.2.

In all experiments, the only variable is the shapes of nozzles, having different number of sharp corners and different angles, to examine the intensity of turbulence through temperature fluctuation.

### B. MEASURING INSTRUMENTS

The following devices are used to measure the flame temperature and flow rates of reactants

#### 1. THERMOCOUPLE:

Temperature is measured locally using S-type thermocouple, with a bead diameter of 0.5 mm, and connected to a digital read out.

Radiation correction is calculated using the following equations:

$$q_c = q_r \quad (1)$$

$$\text{Where: } q_c = h_c \times A \times (T_g - T_p) \quad (2)$$

$$q_r = \varepsilon \times \sigma \times A \times (T_p^4 - T_{p,surr}^4) \quad (3)$$

$$\Delta T = T_g - T_p = (\varepsilon \times \sigma \times T_p^4) / h_c \quad (4)$$

$$h_c = (k/d) \times (2 + 0.6 \times (c_p \times \mu / k)^{0.33} \times (u d \rho / \mu)^{0.5}) \quad (5)$$

#### 2. MANOMETERS:

A u-tube manometer is used to measure air flow rate in the main line, the manometer liquid is colored water with approximate density of 1000kg/m<sup>3</sup>.

An inclined manometer is used to measure the fuel flow rate with the same manometer liquid, with an angle of 60° with the vertical.

Both manometers are attached to two orifices to create a pressure drop.

**3. ORIFICE:**

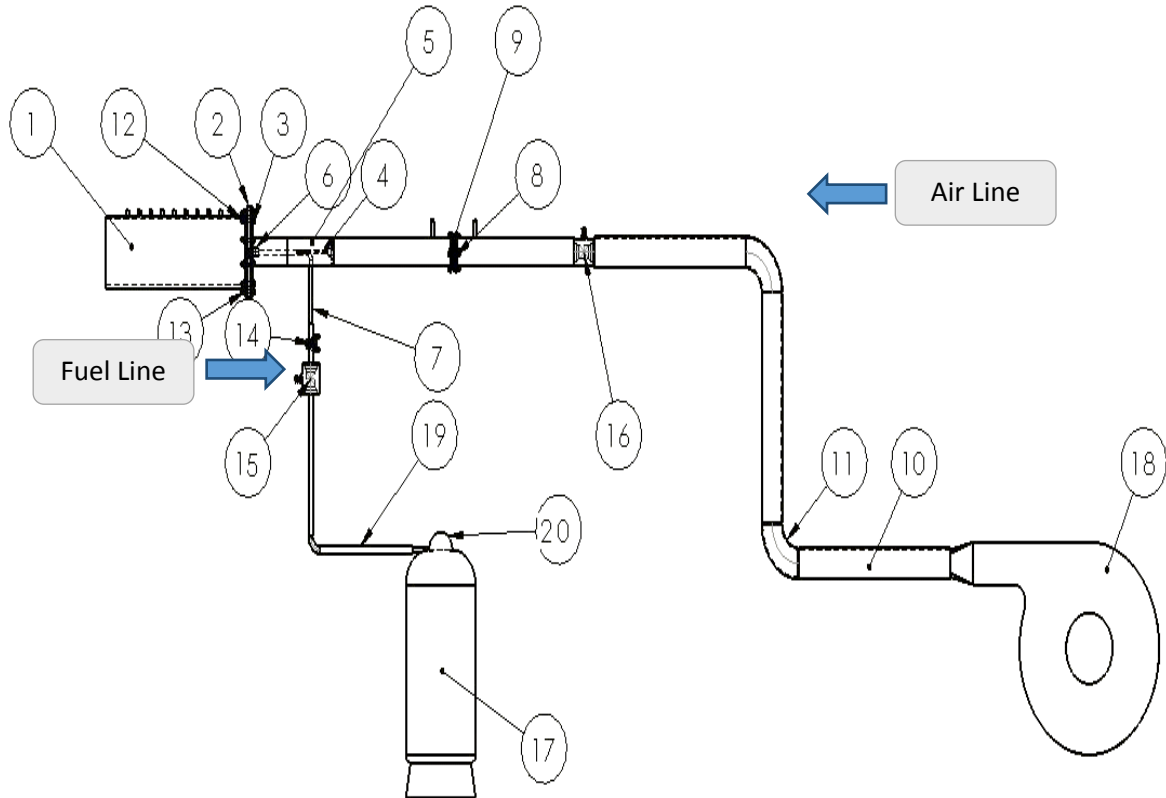
Two orifice plates are used to insure that the air to fuel ratio is constant through the experimental work. An orifice is installed in the main air line of 3 inches diameter part (9) fig. 2, another one of 0.5 inch is installed in the fuel line part (14) fig. 2.

The following equations are used to measure the flow rates:

$$m_A^o = \rho_a C_{dA} A_{Ao} \sqrt{2h_{air}} \quad (6)$$

$$m_F^o = \rho_F C_{dF} A_{Fo} \sqrt{2 \frac{h_f \times g \times \rho_{water}}{\rho_F}} \quad (7)$$

Where:  $C_{dA} = C_{d \text{ air orifice}} = 0.63$   
 $C_{dF} = C_{d \text{ fuel orifice}} = 0.62$   
 $A_{Ao} = A_{\text{air orifice}} = 0.0019 \text{ m}^2$   
 $A_{Fo} = A_{\text{fuel orifice}} = 5.67 \times 10^{-5} \text{ m}^2$   
 $\rho_{fuel} = 2.3 \text{ kg/m}^3$

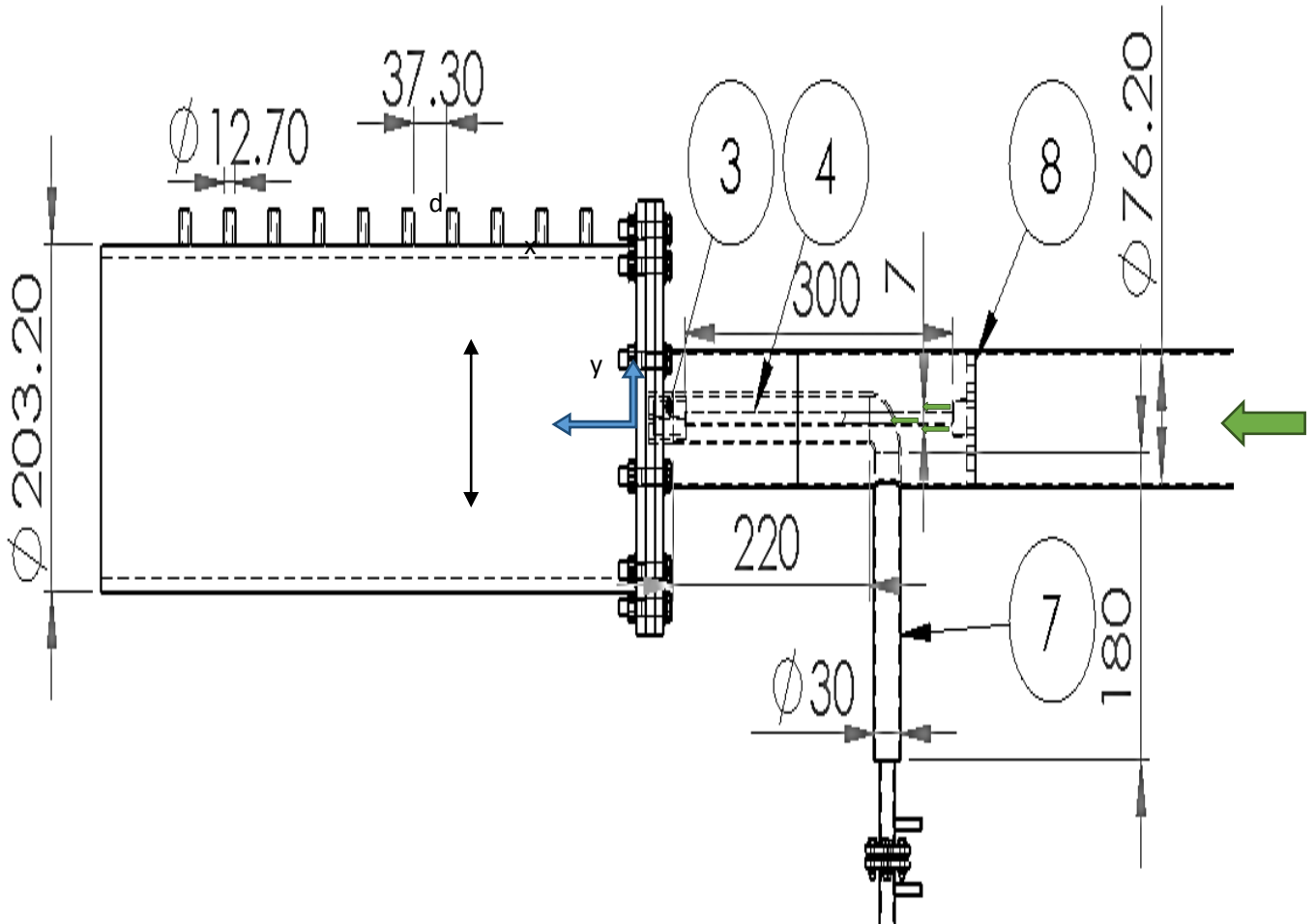


- |  |                                     |                           |
|--|-------------------------------------|---------------------------|
| 1 Combustion Chamber                             | 8 First Air Orifice Meter Assembly  | 15 Fuel Control Valve     |
| 2 Flange for Nozzle Fixation                     | 9 Second Air Orifice Meter Assembly | 16 Air Control Valve      |
| 3 Air End Line                                   | 10 Main Air Delivery Line           | 17 L.P.G.                 |
| 4 Air Distribution Connection and flame arrestor | 11 Elbow 90o 1R for Main Air Line   | 18 Air Blower             |
| 5 Fuel End Line                                  | 12 Ten Ports for Measurements       | 19 Fuel Main Line         |
| 6 Nozzle   | 13 Ten Bolt and Nut M10             | 20 Gas Pressure Regulator |
| 7 Fuel Delivery Line                             | 14 Fuel Orifice Meter               |                           |

Fig. 2: Experimental test rig setup

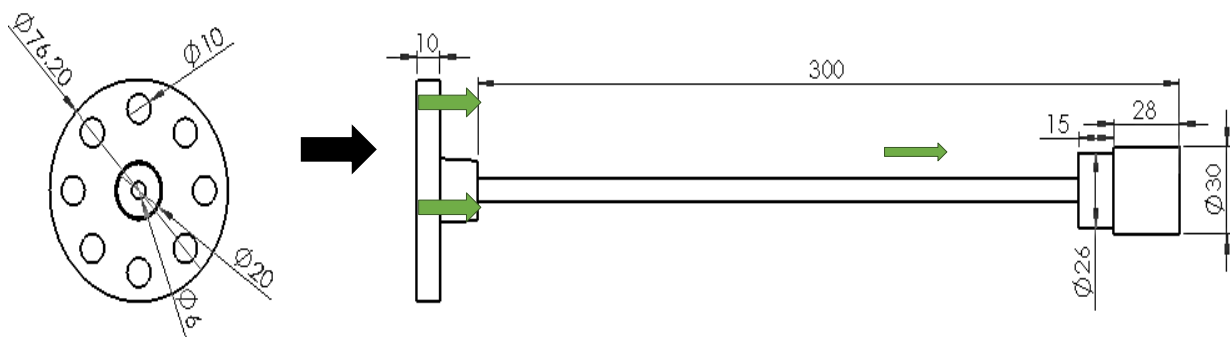
Fig. 3 shows a detailed view of air and fuel passes, air line is a horizontal line having an arrangement of distribution to get a centralized air stream in the center of fuel, using the arrangement in fig. 4, the fuel comes from the vertical

line which is connected to the fuel cylinder and comes out through the nozzles. So the final arrangement of inverse diffusion flame from the center to outside is air-fuel-air.



Note: All dimensions in [mm]

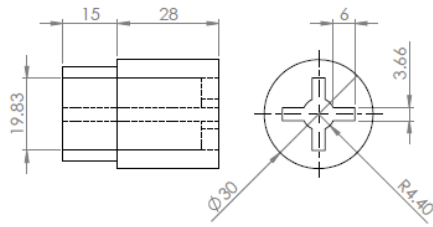
Fig.3: Air/Fuel lines assembly



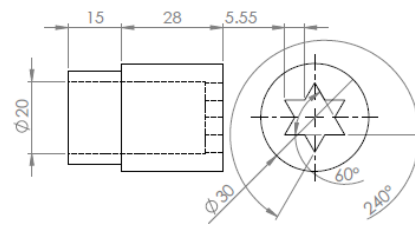
Note: All dimensions in [mm]

Fig.4: Air distribution arrangement

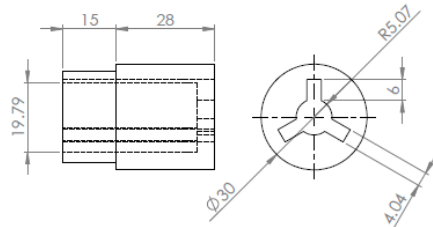
A detailed view of nozzles used in the experiments is showed in fig. 5, showing the angles, nozzle diameter, flat side length and shape of nozzles.



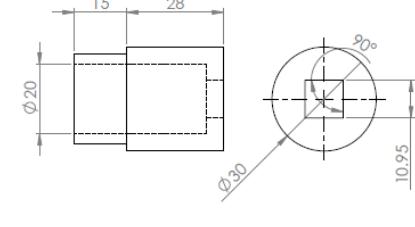
Nozzle (1) - Cross



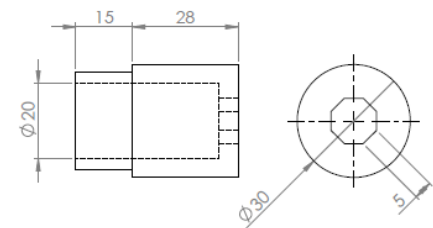
Nozzle (6) - Six Point Star



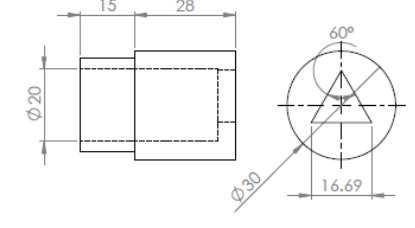
Nozzle (2) Y-Shape



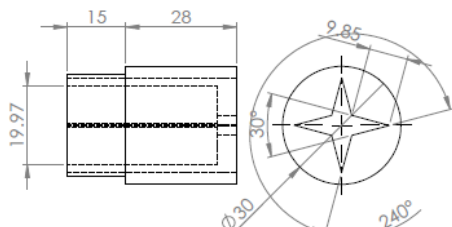
Nozzle (7) - Square



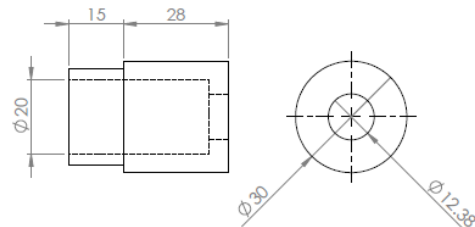
Nozzle(3)- Octagon



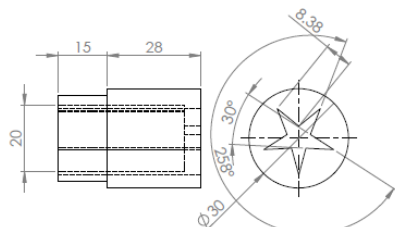
Nozzle (8) - Triangle



Nozzle (4) - Four Point Star



Nozzle (9) - Circle












Nozzle (5) - Five Point Star

Fig. 5: Nozzles Cross Section Details

Note: All dimensions in [mm]

TABLE 1: CROSS-SECTION DETAILS OF FUEL NOZZLES:

Nozzle Number	Shape	Name	Area (mm <sup>2</sup> )	Perimeter (mm)	Number of sharp	Interior vertex angle (°)	Flat side length (mm)
1		Cross	120	65	16	90 & 225 *	4&5
2		Tri-shape	120	62	12	90 & 235 *	4&6
3		Octagon	120	40	8	135	5
4		4-point star	120	80	8	30 & 240	10
5		5-point star	120	85	10	30 & 255	8.5
6		6-point star	120	60	12	60 & 240	5
7		Square	120	44	4	90	11
8		Triangle	120	51	3	60	17
9		Circle	120	39	0	-	-

\* The angle between the straight line and the tangent to the inner circular race of nozzle

III. RESULTS AND DISCUSSION:

A. The effect of nozzle geometry:

In analyzing the results some findings were dedicated, which can help in understanding the effect of the sharp corners in the flow field. Examining the relation of perimeter with the peak temperature of flame as shown in Fig.6, it was found that at perimeter 40 mm and 8 corners (octagon), Fig.7, we achieved the maximum flame temperature, with interior angles of 135°

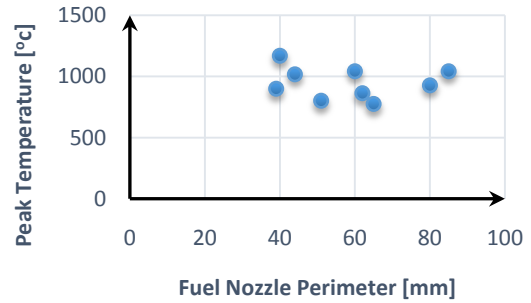


Fig.6: Relation between shapes perimeter in mm and Peak Temperature in °C

It can be seen from Fig.7 that the maximum peak temperature is reached for 8 sharp corners shape as well as another value occur at the same number of corners, and this phenomena was repeated for 12 corners nozzles. This means that there is another variable that should be taken into consideration not only the number of sharp corners. In addition increasing the number of corners to 16 caused a decrease in the peak flame temperature.

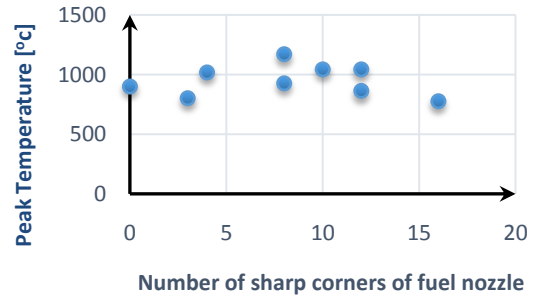


Fig.7: Relation between number of sharp corners in nozzles and Peak Temperature in °C

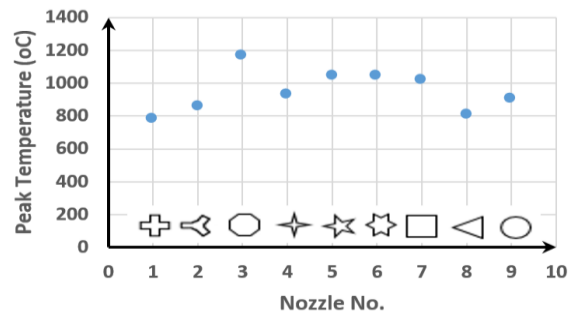


Fig.8: Variation of peak temperature with nine nozzles

Fig.8 shows clearly that the octagonal nozzle no. (3) gives the maximum combustion efficiency while nozzle no.(1) gives the lowest one and this was clear from the maximum temperature recorded for every shape as the air to fuel ratio and nozzles cross-section area are constant with a values of 50.30 as a total

value distributed as 52.06 for outer race of flame and 2.45 for inner race and 120 mm<sup>2</sup> respectively.

Another aspect should be taken into consideration in achieving a turbulent flow is the local temperature fluctuation, and how it is affected with nozzle geometry. This analysis is conducted on averaged temperature bases using the following equation which resulted in the graph shown in fig. 9

$$\text{Temperature Fluctuation} = \sqrt{\frac{\sum(T - T_{avg.})^2}{T_{avg.}}} \quad (8)$$

It is clear that nozzle (4) gives the maximum temperature fluctuation % due to the severe mixing that is taking place in a 30° sharp corner. This causes an interaction of boundary layers, and meanwhile it produces stagnation points causing wakes and turbulence production sites, as demonstrated by [10]. However, Increasing the number of sharp corners increases the number of turbulence production sites, while the smaller vertex angles settled a more severe potential for flow strain around the corner as illustrated by (Kamal, 2013), [1].

In comparing the results to the circular nozzle it is found that nozzle (4) has 85.61% more temperature fluctuation.

It was also noticed that the square nozzle number (7) showed fluctuation that is less than the value achieved by the circular nozzle, regarding the corners, this shape has got a 90° angles with four stagnation points only, which may reflect the reason behind the low fluctuation in temperature.

The flame length highly effects the industry, and it is favorable to get a short flame with a maximum temperature, but the property of inverse diffusion flame has a very important role in cooling the flame centrally, which could be good at decreasing the NOx emissions.

It is clear from fig.10 that the triangular nozzle produces the shortest nozzle in comparing to the circular one, with a 50% reduction in length.

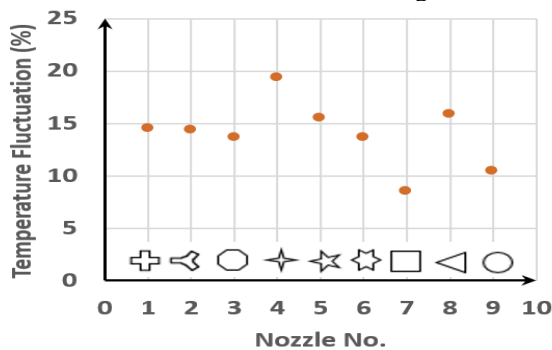


Fig. 9: variation of average temperature fluctuation in % with the nine nozzles

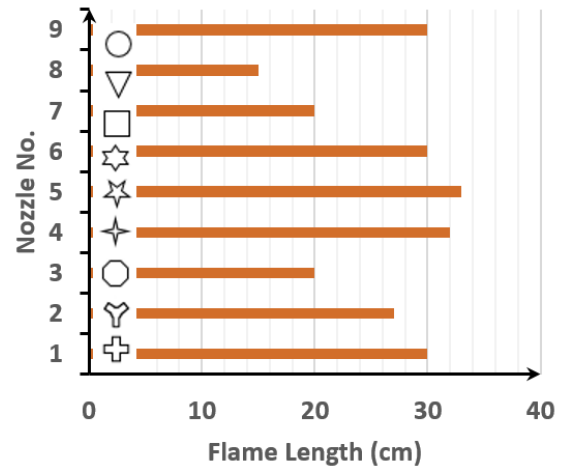


Fig.10: Variation of Flame Length with the nine nozzles

### B. Temperature analysis

The analysis of experimental results is carried out using two streams, the radial analysis at every constant cross-section and the axial analysis at constant horizontal plans.

#### i. Radial analysis of temperature distribution:

Figures 11 through 16 show the relations between radial position (y/d) and the average temperature at different axial measuring points (x/d) from the nozzle, they show a wide change in local temperature distribution.

A simple analysis of the graphs showed the homogeneity of temperature distribution as shown in table (2), and it is found that in fig.11, the peak temperature using the cross nozzle no.(1) increased by 90% from the peak value recorded by the circular nozzle no.(9) at the same position (x/d = 0.025), moreover the flame conducted from nozzles no. 3,6,7 and 8 reaches the maximum value all-over the entire flame, which means that the flame reached the core envelop at this distance.

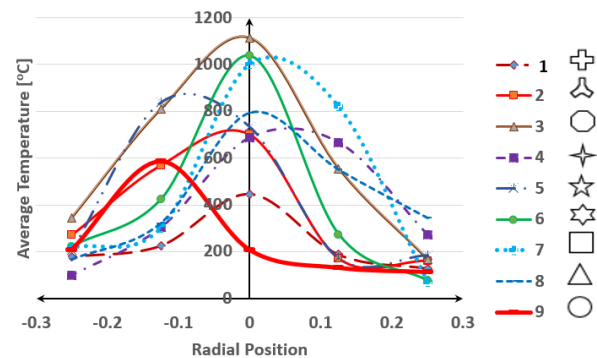
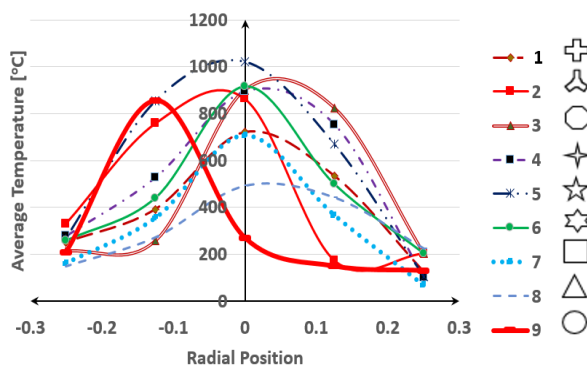


Fig. 11: The relation between radial position y/d and the average temperature at x/d=0.025 from the nozzle

**TABLE 2: TEMPERATURE DISTRIBUTION ANALYSIS THROUGH DIFFERENT FUEL NOZZLES:**

Fig. no.#	x/d	type	Nozzle no.#
11	0.025	Symmetric	1,3,6
		Over center	4,7,8
		Under center	2,5,9
12	0.05	Symmetric	6,7,5
		Over center	1,3,4,8
		Under center	2,9
13	0.075	Symmetric	6,9,1
		Over center	3,5,7,8
		Under center	2,4
14	0.1	Symmetric	9,2,4,5,3,6
		Over center	7
		Under center	1
15	0.123	Symmetric	2,5
		Over center	4,6,9
		Under center	1
16	0.197	Symmetric	5,9,6,2
		Over center	4
		Under center	1

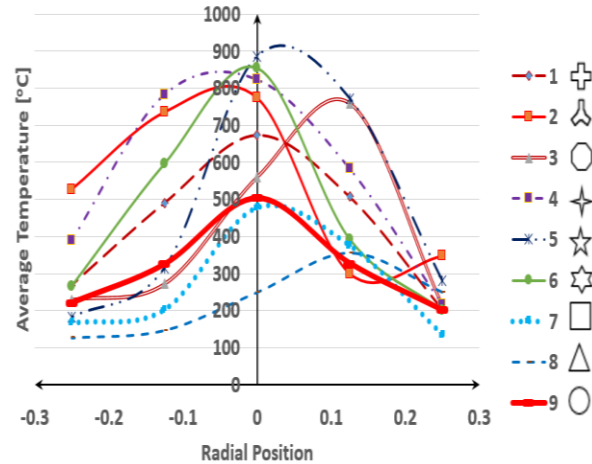
In comparing fig.11 and 12, the relation between radial position  $y/d$  and the average temperature at  $x/d=0.049$  from the nozzle is recorded, and it is clear that the flame starts to develop and make a homogeneous temperature distribution, also the peak temperature is reached for nozzles no.1, 2, 4, 5 and 9 which means that the position of the flame core is shifted upstream and the flame length increase searching for oxygen to complete combustion. This concept is achieved through all nozzles except nozzle no. (6), 6-point star, which have a perimeter of 60mm, 12 sharp corners, angles of  $60^\circ$  and  $240^\circ$  and a flat side length of 5mm. in comparing nozzle (6) with the circular nozzle no. (9) it is found that the flame length is of the same value but the peak temperature in nozzle (6) is 21.26% higher than the circular one. This is due to the presence of sharp angles in flow field of flame.



**Fig. 12: The relation between radial position  $y/d$  and the average temperature at  $x/d=0.049$  from the nozzle**

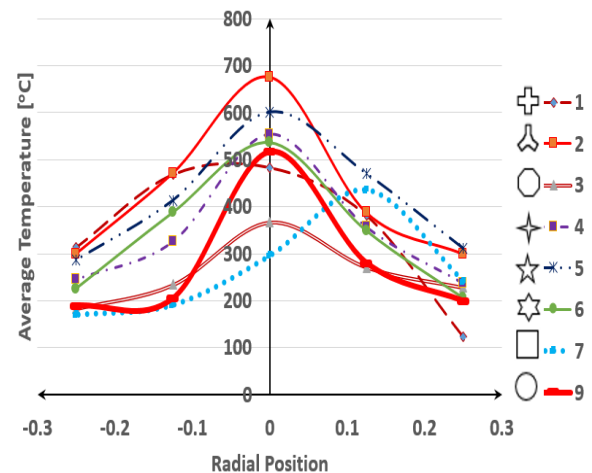
Fig.(13) shows a reduction in flame temperature for all nozzles, all nozzles are having the same trend except the circular nozzle which takes the symmetric attitude.

Disturbance takes place again which means that there is turbulence in flow field and the entrainment of air from the outer race takes place.



**Fig. 13: The relation between radial position  $y/d$  and the average temperature at  $x/d=0.075$  from the nozzle**

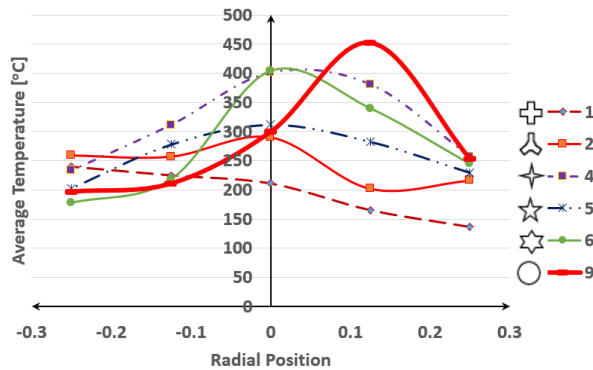
Starting  $x/d = 0.1$ , fig. 14, the flame propagated from nozzle (8) disappeared and the majority of flames takes the symmetric trend, which means that the flames attain homogeneity again



**Fig. 14: The relation between radial position  $y/d$  and the average temperature at  $x/d=0.1$  from the nozzle**

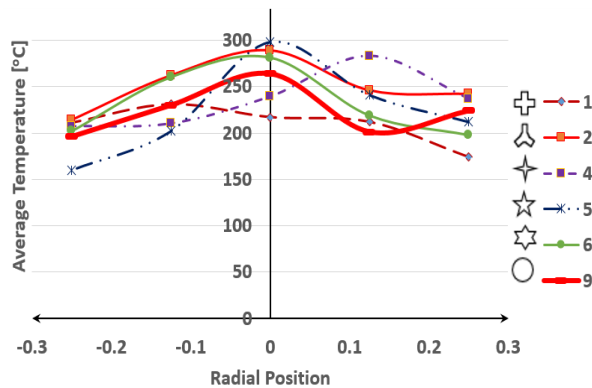


At  $x/d = 0.123$ , fig. 15, Nozzle (9) shows a severe change in temperature at the upper part of flame, and flames from nozzles (3 and 7) also disappeared, circular nozzle lost its symmetry again to declare a fluctuation in temperature due to mixing from inverse jet of air in the center of fuel jet.



**Fig. 15:** The relation between radial position  $y/d$  and the average temperature at  $x/d=0.123$  from the nozzle

At  $x/d=0.197$ , fig. 16, the curves are flattened and the differences in temperature is not great, which means that the flame length in reached thermally, and the temperature of flue gases is homogeneous and reached the favored mixing condition.

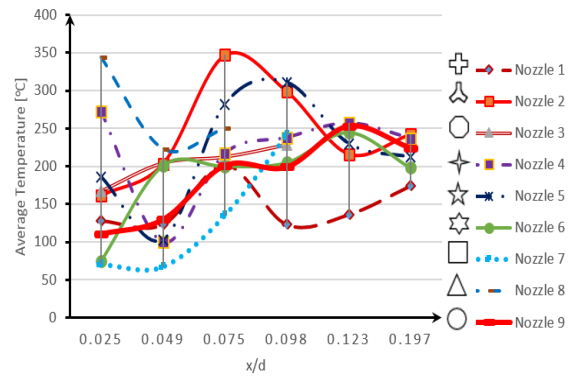


**Fig. 16:** The relation between radial position  $y/d$  and the average temperature at  $x/d=0.197$  from the nozzle

**ii. Axial analysis of temperature distribution:**

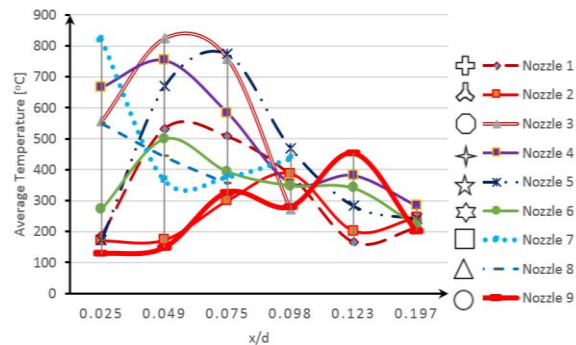
Figures 17 through 21, shows the relation between axial position ( $x/d$ ) and the average temperature at different radial positions ( $y/d$ ), and it is clear that the temperature trend reaches the peak values for all the nozzle at the center line of combustor ( $y/d=0$ ) as shown infig.19. All the charts show a high temperature difference and the nozzle

surface then this value decays along flame axial length, except at ( $y/d=-0.25$ ), Fig. 21, where the flames reach the maximum temperature difference at ( $x/d=0.075$ ) then the difference decay as usual.



**Fig. 17:** The relation between axial position  $x/d$  and the average temperature at  $y/d=0.25$

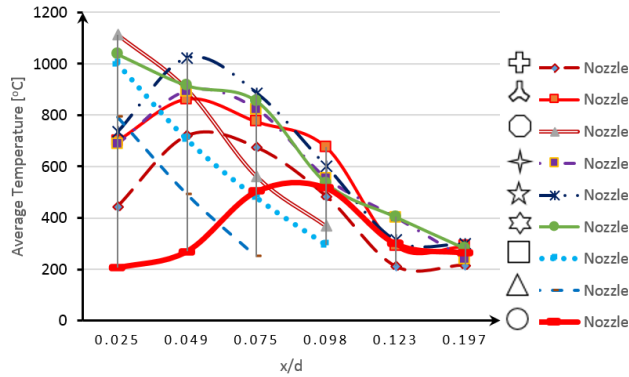
At  $y/d = 0.25$  and  $0.125$ , Figures17 and 18, there is a violent changes in temperature , these changes reflects the effect of mixing and interaction of boundary layers and it was expected to find a symmetric trend beneath the centerline of flame , but this was not achieved due to the buoyancy forces which aims to lift the flame.



**Fig. 18:** The relation between axial position  $x/d$  and the average temperature at  $y/d=0.125$

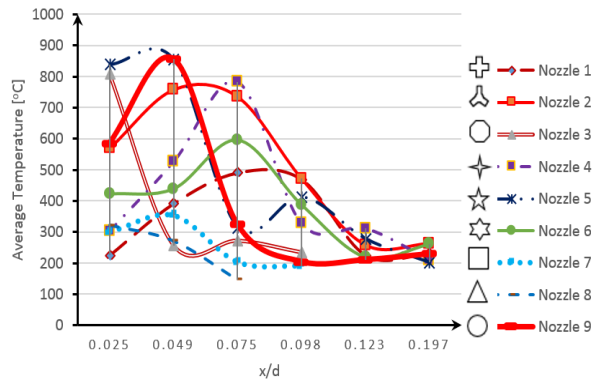
The bell shape is taken as a trend for the temperature distribution, and the shapes that didn't give the same shape probably means that the measuring points were not enough and needs to reduce the gaps of reading points.

Fig. 20 shows a sudden change in temperature for the circular nozzle, while the square nozzle temperature is decreased at a range of  $700\text{ }^{\circ}\text{C}$  from the values recorded at  $y/d = 0.125$ , in fig. 19.



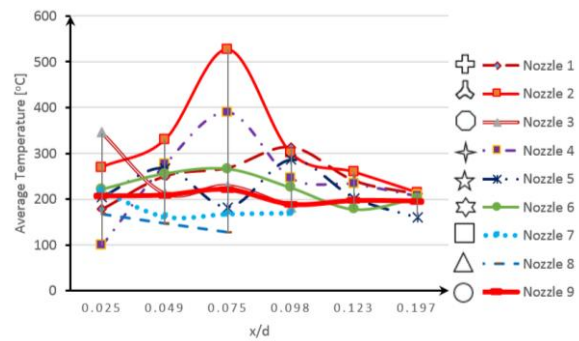
**Fig. 19: The relation between axial position  $x/d$  and the average temperature at  $y/d=0$**

Through all curves of axial temperature distribution, it is noticed that there is no flame for nozzle no. (8) starting  $x/d = 0.075$ , and nozzles no. (3 and 7) starting  $x/d = 0.098$ , this result agree with the measurement of length done in fig. 10, on the other hand, it is expected that the flame of nozzle no. (2) extinguish by  $x/d = 0.098$  but the thermal measurement of flame length showed its continuity. This could be due to mixing produced as a result of sharp corners geometry.



**Fig. 20: The relation between axial position  $x/d$  and the average temperature at  $y/d=-0.125$**





The photos, table (2) show visual flame length and volume, as well as flame spectrum, and it is noticed that nozzle no. (1) gives the longest flame and most orange flame, on the other hand nozzle no. (4) gives the shortest flame length with a favorable bluish flame. Concerning flame volume, the volume is calculated approximately by measuring the flame length and taking the flame diameter as a constant value, so the flame length here is used as an indication to the flame volume. nozzle no. (6) gives the maximum volume, which means better mixing and attachment, while nozzle no. (8) has the minimum volume.





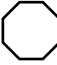


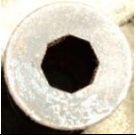












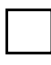







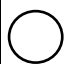





**Fig. 21: The relation between axial position  $x/d$  and the average temperature at  $y/d=-0.25$**

It is observed from the photos in table (2) that the base of the flame in all nozzles is blue and the entire flame is grading orange, this is due to the excess oxygen at  $x$  and  $y$  equal zero, also due to the enlargement that takes place through the combustor body, which leads to high friction in flow and consequently a better mixing zone

**TABLE 2: EXPERIMENTAL RESULTS**

Nozzle Number	Shape	Peak Temperature (°C)	Flame Length (cm)	Maximum Temperature Fluctuation (%)	Averaged Temperature Fluctuation (%)	Isometric View Photos of Flames	Side View Photos of Flames	Nozzle Photo
1		776	30	42.73	14.45			

2		863	27	39.97	14.31			
3		1170	20	97.93	13.65			
4		927	32	92.90	19.36			
5		1043	33	43.48	15.51			
6		1043	30	18.24	13.65			
7		1018	20	33.05	8.54			
8		802	15	45.22	15.9			
9		900	30	16.22	10.43			

#### IV. CONCLUSIONS

All nozzles are compared to the circular nozzle, and it is found that at the same location all sharp corners nozzles showed higher temperature than the reference value.

The results of the experimental work that was discussed before are concluded in the following points:

- Nozzle number (9), circle, produced a long flame of 30 cm with orange color and peak temperature of 900°C, which means that the combustion is incomplete.
- Nozzle number (4), 4-point star, has very high sharpness of acute angles, which leads to a high maximum temperature fluctuation, which in fact causes a noisy effect.
- Nozzle number (3), Octagon, gave the maximum temperature, but with low turbulence due to obtuse angles in the shape.
- Nozzle number (1), Cross, the shape of the nozzle has the highest number of vertices that caused the best mixing of reactants to get the lowest peak temperature.
- Nozzle number (7), Square, recorded the least temperature fluctuation.

#### REFERENCES

- [1] M.M.Kamal, "A comparative study of the port geometrical effects on sharp corners' jet triple flames," *Exp. Therm. Fluid Sci.*, vol. 51, pp. 149–163, 2013.
- [2] J.Mi and G. J. Nathan, "Statistical properties of turbulent free jets issuing from nine differently-shaped nozzles," *Flow, Turbul. Combust.*, vol. 84, no. 4, pp. 583–606, 2010.

- [3] S.Lee, P. Lanspeary, G. Nathan, R. Kelso, and J. Mi, "Preliminary study of oscillating triangular jets," 14th Australas. Fluid Mech. Conf., no. December, pp. 821–824, 2001.
- [4] W.R.Quinn, "Phase-averaged measurements in an isosceles triangular turbulent free jet," *Exp. Fluids*, vol. 39, no. 5, pp. 941–943, 2005.
- [5] S.R.Gollahalli and Samir Subba, "Partially premixed laminar gas flames from triangular burners," *J. Propuls. Power*, vol. 13, no. 2, pp. 226–232, 1997.
- [6] E.J.Gutmark, F.F. Grinstein, "Flow control with noncircular jets", *Annual Revised Fluid Mechanics* 31, 239–272, 1999.
- [7] C.O.Iyogun and M. Birouk, "Effect of fuel nozzle geometry on the stability of a turbulent jet methane flame," *Combust. Sci. Technol.*, vol. 180, no. 12, pp. 2186–2209, 2008.
- [8] K.Wohl, C. Gazley, and N. Kapp, "Diffusion flames. 3rd Symposium on Combustion and Flame and Explosion Phenomena", Baltimore, MD, 288, 1949.
- [9] L.Vanquickenborne, and Van Tiggelen, A. "The stabilization mechanism of lifted diffusion flames", *Combust. Flame*, 10, 59–69, 1966.
- [10] H.Schlichting, "Boundary -layer theory", German: McGRAW-HILL BOOK COMPANY, 1970.
- [11] Ahuja A, Manes J, Massey K. "An evaluation of various concepts of reducing supersonic jet noise". AIAA Pap. 90–3982, 1990.
- [12] E.J.Gutmark, K.C. Schadow, T.P. Parr, D.M. Hanson-Parr, K.J. Wilson, "Noncircular jets in combustion systems", *Experiments Fluids* 7 ,248–258, 1989.
- [13] E.Gutmark, K.C. Shadow, K.J. Wilson, "Subsonic and supersonic combustion using noncircular injectors", *Journal of Propulsion Power* 7, 240–249, 1991.
- [14] W.R.Quinn, "On mixing in an elliptic turbulent free jet", *Physics of Fluids A* 1,1716–1722, 1989.
- [15] W.R.Quinn, "Upstream nozzle shaping effects on near field flow in round turbulent free jets", *European Journal of Mechanics B/Fluids* 25, 279–301, 2006.
- [16] S.R.Gollahalli, S. Subba, "Partially premixed laminar gas flames from triangular burners", *Journal of Propulsion Power* 13, 226–232, 1997.
- [17] W.R.Quinn, "Streamwise evolution of a square jet cross section", *AIAA Journal* 30, 2852–2857, 1992.
- [18] W.R.Quinn, "Measurements in the near flow field of an isosceles triangular turbulent free jet", *Experiments Fluids* 39, 111–126, 2005.
- [19] V.Piffaut "Axis Switching in Square Co-Axial Jets", MSc Thesis, Louisiana State University, USA, 2003.
- [20] S.Bonnafoous, "Experimental Study on Passive and Active Control of Co-Axial Turbulent Jet", MSc Thesis, Louisiana State University, USA, 2001.
- [21] T.F.Fric, A. Roshko, "Vortical structure in the wake of a transverse jet", *Journal of Fluid Mechanics* 279, 1–47, 1994.
- [22] E.J.Gutmark and F. F. Grinstein, "Flow Control With Noncircular Jets," *Annu. Rev. Fluid Mech.*, vol. 31, pp. 239–272, 1999.
- [23] K.Serkh and V. Rokhlin, "On the solution of elliptic partial differential equations on regions with corners," *J. Comput. Phys.*, vol. 305, pp. 150–171, 2016.
- [24] R.Azzoni, S. Ratti, S. K. Aggarwal, and I. K. Puri, "The structure of triple flames stabilized on a slot burner," *Combust. Flame*, vol. 119, no. 1–2, pp. 23–40, 1999.
- [25] J.Hart, J. Naser, and P. Witt, "Coherent structure dynamics in jets from irregular shaped nozzles," 15th Australas. Fluid Mech. Conf. Sydney, Aust., no. December, pp. 1–4, 2004.